Proc. of the 5th WSEAS/IASME Int. Conf. on Electric Power Systems, High Voltages, Electric Machines, Tenerife, Spain, December 16-18, 2005 (pp68-73)

Control of Synchronous Motors using the Causal Ordering Graph, Part I: Model Description

Ghislain REMY, Pierre-Jean BARRE, Philippe DEGOBERT, Jean-Paul HAUTIER
Laboratory of Power Electronics and Electrical Engineering of Lille (L2EP)
Technological Research Team – ERT CEMODYNE
ENSAM, 8 Bd Louis XIV, 59046 Lille Cedex
FRANCE
barre@lille.ensam.fr http://www.lille.ensam.fr/cemodyne

Abstract: - This paper is Part I of a two-part article. The control design of synchronous motors is now classical, so it is helpful to present graphical tools of control design such as the Causal Ordering Graph (COG). In Part I, we present classical models of permanent magnet synchronous motors using the COG. These models are developed and analysed in the stationary reference frame, in Concordia's reference frame and in Park's reference frame. The Causal Ordering Graph representation of models reveals the nature of the interactions between currents and fluxes. Also, the torque expression of synchronous motors is presented as a non-bijective relation. In order to establish nonspecific models, an analogy between rotary and linear synchronous motor is presented. Afterwards, the specificities of linear motors are exposed. This property of models will be taken into account to generate controllers using the inversion principle of COG in Part II.

Key-Words: - Causal Ordering Graph, Rotary Synchronous Motor, Linear Synchronous Motor, Modelling.

1 Introduction

The purpose of this paper is to establish generic models of synchronous motors using the Causal Ordering Graph (COG) in order to establish the optimal control structures of such systems. Nowadays, numerous modelling techniques are available: Finite elements models, self-tuning parameters models, state space formalism, *etc* [1]. Nevertheless, some of these models cannot be used directly inside control structures, because of: buffer size limitation, maximum value of CPU turnaround time, and so on [2]. In this paper, we apply the COG formalism to a synchronous motor because it takes into account the causal behaviour of physical phenomena. In fact, the COG is a descriptive method, which helps to discern the causality of a system [3]. This property becomes truly important to elaborate control strategies for maintaining the torque control.

After explaining the principle of the Causal Ordering Graph, we apply this methodology to simplified models of synchronous motors in (α-β) Concordia's reference frame and in (d-q) Park's reference frame. The (abc) stationary reference frame gives a so-called natural model, whereas (α-β) Concordia's transformation gives a so-called generalised model. (d-q) Park's reference frame, known as the synchronous reference frame, gives constant values of corresponding currents and fluxes in the direct axis and quadrature axis only. Furthermore, as we develop a generic model, an analogy between rotary and linear synchronous motors is made. The specificities of linear motors are exposed in order to obtain more accurate models.

In Part II, the inversion principle of the COG is applied so as to build an optimal control structure. Thus, examples of vector control strategies in Concordia's reference frame and in Park's reference frame are given; they are validated with experimental results on a linear synchronous motor.

2 The Causal Ordering Graph: Model

2.1 The COG specificities

System modelling aiming to design optimal controllers is a classical engineering approach. But only systematic methods guarantee the successful study of the complex system analysis. The Causal Ordering Graph is a systematic method based on a located energy representation with the theory of causal ordering [3-6].

It is undeniable that this approach is connected with that of links graphs such as the Bond Graphs [7-11]. But it differs from them by the analysis process, which is based on integral causality only. The COG is a tool that structures the synthesis of a state model, but that aims at maintaining, for a given system, a representation as close as possible to that felt in the observation. Obviously, the resulting model will be affected by the neglected elements as well as the explicit and implicit assumptions induced by the physical interpretation of the constitutive objects. Lastly, the fundamental objective of the COG tool is to propose, by a graphical method and thanks to some simple principles, a synthesis of the control law taking into account the physical transfers of the process.

2.2 The Causal Ordering Graph principle

The Causal Ordering Graph is built up with several graphical processors attached to different objects located in the studied process. The evolution of these objects is characterized by a transformation relation between influencing quantities and influenced quantities. This relation is induced by the principle of causality governing the energetic relation of an object or group of objects. In short, the output of a processor only depends on present or past values of the inputs. Such a formulation expresses the causality in integral form, and this concept is illustrated by many significant electrical and mechanical examples. Since the flux in a self is an integral function of the voltage, by analogy, the kinetic moment of a rigid mass is the integral function of the applied efforts. The electricity quantity in a capacitor is an integral function of the current; by analogy, the endpoints position of a spring is the integral of the velocity variation between the endpoints (Hooke's law) [12].

In general, the expression of the transformation relations by means of the state equations is the best warranty against physical misinterpretation. To simplify the presentation, we will only retain two complementary definitions of integral causality: (Fig.1.a) If an object accumulates information, causality is internal: the output is necessarily a function of the energy state. The relation, thus oriented, is known as causal. Time and the initial state are implicit inputs and are not represented (Fig.1.b). On the contrary, if an object does not accumulate information, causality is external. The output is an instantaneous function of the input. The relation, which is not oriented, is then known as rigid. Fig.1 gives the selected symbolism to differentiate between the two kinds of processors.

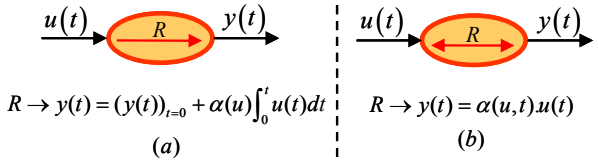

Fig.1: COG symbolisms:
(a) causal relation, (b) rigid relation.

3 Model of Synchronous Motors

3.1 Assumptions and definitions

To focus the work presented here, the following assumptions are made:

1) Only three-phase motors are considered.
2) Motors are star-connected with an inaccessible neutral wire.
3) All three phases are balanced, so the electrical angle of each current is shifted by 2π/3 from that of each other.
4) The same goes for non-sinusoidal back-EMF.
5) Resistances and inductances of the three phases are identical and constant.
6) The magnetic circuit is not saturated.
7) Slot effects are taken into account as cogging force with its first harmonic value.
8) Magnetomotive forces are considered to have a sinusoidal space repartition.

Depending on construction, materials and rotor design, we can classify the synchronous motors in four basic groups: reluctance motors, hysteresis motors, electromagnetically-excited motors, and permanent magnet (PM) motors [13-14]. At this point, the study is restricted to PM motors only. The polyphase synchronous motor considered has three pole pairs. The rotor is made of surface-deposed permanent magnets. Fig.2 gives a scheme of the permanent magnet synchronous motor (PMSM) studied.

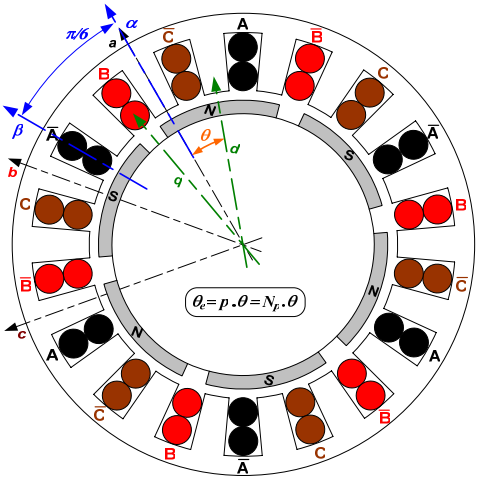

Fig.2: Schematic view of the studied PMSM

Consequently, we can apply additive properties on fluxes and currents. Then, axes are defined in the electrical frame, where $\theta_e = N_p \cdot \theta$.

Three identical windings in the stator are separated from each other with an electrical angle of $2\pi / 3$. The axis of phase *a* defines the (*abc*) stationary reference frame, Fig.2.

Moreover, the *a* axis also represents the direct axis α of Concordia's reference frame. The quadrature axis β of Concordia's reference frame is separated by a mechanical angle of $\pi / 6$ from its direct axis α. Concordia's reference frame is a so-called diphase stationary reference frame.

Inside the rotor, the direct axis *d* of Park's reference frame is defined in the middle of a north permanent magnet. Then, the quadrature axis *q* of Park's reference frame is separated by a mechanical angle of $\pi / 6$ from its direct axis *d* (the same as an electrical angle of $\pi / 2$). Park's reference frame is a so-called synchronous reference frame.

3.2 The *abc* stationary reference frame

Equations of the electrical part of synchronous motors are depicted as follows:

$$[R_{abc}]=\begin{bmatrix} R & 0 & 0 \\ 0 & R & 0 \\ 0 & 0 & R \end{bmatrix},\quad [L_{abc}]=\begin{bmatrix} L & M & M \\ M & L & M \\ M & M & L \end{bmatrix} \tag{1}$$

$$\begin{bmatrix} V_a \\ V_b \\ V_c \end{bmatrix}=[R_{abc}]\cdot\begin{bmatrix} i_a \\ i_b \\ i_c \end{bmatrix}+[L_{abc}]\frac{d}{dt}\begin{bmatrix} i_a \\ i_b \\ i_c \end{bmatrix}+\omega.N_p\frac{d}{d\theta_e}\begin{bmatrix} \phi_a \\ \phi_b \\ \phi_c \end{bmatrix} \tag{2}$$

$$T_{em}\cdot v = e_a\cdot i_a + e_b\cdot i_b + e_c\cdot i_c \tag{3}$$

Fig.3 presents the Causal Ordering Graph of the electrical part in the stationary reference frame. The COG relations of Fig.3 show that balanced conditions give a symmetrical graph, and explain that phases can be represented as a simplified vector scheme.

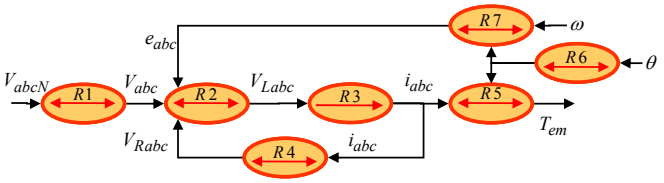

Fig.3: COG of the electrical part of a PMSM in (*abc*)

The different relations are given by:

$$R2 \rightarrow V_{Labc} = V_{abc} - e_{abc} - V_{Rabc}$$

$$R3 \rightarrow (L-M)\frac{d}{dt}i_{abc} = V_{Labc}$$

$$R6 \rightarrow \begin{cases} \dfrac{d\phi_a}{d\theta} = N_p.\hat{\phi}_f \sin(N_p\cdot\theta) \\ \dfrac{d\phi_b}{d\theta} = N_p.\hat{\phi}_f \sin(N_p\cdot\theta - 2\pi/3) \\ \dfrac{d\phi_c}{d\theta} = N_p.\hat{\phi}_f \sin(N_p\cdot\theta - 4\pi/3) \end{cases}$$

$$R5 \rightarrow T_{em} = i_a\cdot\frac{d\phi_a}{d\theta} + i_b\cdot\frac{d\phi_b}{d\theta} + i_c\cdot\frac{d\phi_c}{d\theta}$$

$$R7 \rightarrow e_{abc} = \omega\cdot\frac{d\phi_{abc}}{d\theta}$$

Because of the assumptions taken about the inductances and mutual inductances, the inductance voltage V_L of the $R3$ processor corresponds to an equivalent voltage for the L-M inductance, which represents a part of the energy stored in the system.

The R1 processor represents a matrix transformation used to duplicate the effects of a non-distributed neutral wire, especially the elimination homopolar components and currents with harmonic ranks that are multiples of three.

Next, the mechanical model of the motor can be represented as:

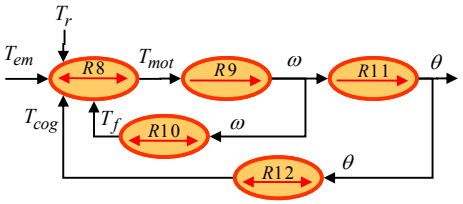

Fig.4: COG of the mechanical part of a PMSM

The different relations are given by:

$$R8 \rightarrow T_{mot} = T_{em} - T_r - T_f - T_{cog}$$

$$R9 \rightarrow J\cdot\frac{d}{dt}\omega = T_{mot},\quad R11 \rightarrow \left(\frac{d}{dt}\right)\theta = \omega$$

$$R12 \rightarrow T_{cog} = \hat{T}_{cog}\cdot\sin(6N_p\cdot\theta)$$

The $R10$ processor represents friction phenomena, which are non-linear. Depending on the control strategy, if speed control is needed at a high speed, viscous friction and Coulomb's friction should be taken into account. Otherwise, if speed control is needed at a low speed, Stribeck's phenomenon could be included, for example [15].

The $R12$ processor represents the cogging forces induced by the interaction between the PMs mounted on the rotor and the stator anisotropy, due to the slotting. According to the stator design of Fig.2, the cogging forces frequency is six times that of the current frequency [16]. However, motors with closed slots or slotless stators are not affected by cogging torque.

As noticed in the COG relations of Fig.4, all the relations are independent of electrical reference frames. So, the mechanical model of a PMSM will be exactly the same in the next developments.

3.3 The *α-β* diphase stationary reference frame

Most of contemporary industrial applications with synchronous motors are made of three-phase windings, which are star-connected with an inaccessible neutral wire. This means that the homopolar component is eliminated. Furthermore, the three currents are linked. Consequently, only two supplied voltages are truly needed to control the PMSM. So, we apply (*α-β*) Concordia's reference frame to (1-3) [17]. Concordia's transformation is defined by:

$$[f_{abc}]=[C_3]\cdot[f_{\alpha\beta 0}],\ with\ C_3=\sqrt{\frac{2}{3}}\cdot\begin{bmatrix} 1 & 0 & 1/\sqrt{2} \\ -1/2 & \sqrt{3}/2 & 1/\sqrt{2} \\ -1/2 & -\sqrt{3}/2 & 1/\sqrt{2} \end{bmatrix}$$

$$[f_{\alpha\beta 0}]=[C_3^{-1}]\cdot[f_{abc}],\ with\ C_3^{-1}=\sqrt{\frac{2}{3}}\cdot\begin{bmatrix} 1 & -1/2 & -1/2 \\ 0 & \sqrt{3}/2 & -\sqrt{3}/2 \\ 1/\sqrt{2} & 1/\sqrt{2} & 1/\sqrt{2} \end{bmatrix} \tag{4}$$

We can define a Causal Ordering Graph of the electrical part in the diphase stationary reference frame, Fig.5.

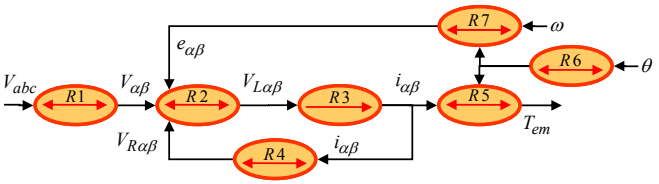

Fig.5: COG of the electrical part of a PMSM in (α-β)

The different relations are given by:

$$R2 \rightarrow V_{L\alpha\beta} = V_{\alpha\beta} - V_{R\alpha\beta} - e_{\alpha\beta},\ R4 \rightarrow V_{R\alpha\beta} = R \cdot i_{\alpha\beta}$$

$$R3 \rightarrow \left(L_{\alpha\beta} \frac{d}{dt} \right) \cdot i_{\alpha\beta} = V_{L\alpha\beta},\ R7 \rightarrow e_{\alpha\beta} = \omega \cdot \frac{d\phi_{\alpha\beta}}{d\theta}$$

$$R5 \rightarrow T_{em} = i_\alpha \cdot \frac{d\phi_\alpha}{d\theta} + i_\beta \cdot \frac{d\phi_\beta}{d\theta}$$

$$R6 \rightarrow \frac{d\phi_{\alpha\beta}}{d\theta} = \sqrt{\frac{3}{2}} \cdot N_p \cdot \hat{\phi}_f \begin{bmatrix} -\sin(N_p \cdot \theta) \\ \cos(N_p \cdot \theta) \end{bmatrix}$$

Wherein:

$$[L_{\alpha\beta}] = \begin{bmatrix} L_\alpha & 0 \\ 0 & L_\beta \end{bmatrix},\ with\ \ L_\alpha = L_\beta = L - M \tag{5}$$

The COG of the electrical part of a PMSM in Fig.5 is a simplified vector scheme. Indeed, we can notice that the diphase machine is equivalent to two elementary independent machines which are mechanically linked. Each one is defined by a flux axis in quadrature with a current axis:

$$T_{em} = \sqrt{\frac{3}{2}} \cdot N_p \cdot \hat{\phi}_f \left[\cos(\theta_e) \cdot i_\beta - \sin(\theta_e) \cdot i_\alpha \right] \tag{6}$$

To be more precise on the behaviour of each fictive machine, we analyse the COG at a rated angular speed: $\theta_e = \omega_e \cdot t = N_p \cdot \omega \cdot t$. So, we have the following equations:

$$\begin{cases} \phi_\alpha = \sqrt{3/2} \cdot \hat{\phi}_f \cos(N_p \cdot \theta) \\ \phi_\beta = \sqrt{3/2} \cdot \hat{\phi}_f \sin(N_p \cdot \theta) \end{cases} \tag{7}$$

$$\begin{cases} e_\alpha = \hat{E} \cos(\omega t + \pi/2) \\ e_\beta = \hat{E} \cos(\omega t) \end{cases},\ \ \hat{E} = \sqrt{3/2} \cdot N_p \cdot \hat{\phi}_f \cdot \omega \tag{8}$$

$$\begin{cases} i_\alpha = \hat{I} \cos(\omega t + \Psi + \pi/2) \\ i_\beta = \hat{I} \cos(\omega t + \Psi) \end{cases} \tag{9}$$

Finally, by transforming (6) and (9):

$$\begin{cases} T_\alpha = \sqrt{3/2} \cdot N_p \cdot \hat{\phi}_f \cdot \frac{\hat{I}}{2} \left(\cos(\Psi) - \cos(2\omega t + \Psi) \right) \\ T_\beta = \sqrt{3/2} \cdot N_p \cdot \hat{\phi}_f \cdot \frac{\hat{I}}{2} \left(\cos(\Psi) + \cos(2\omega t + \Psi) \right) \end{cases} \tag{10}$$

It appears that each elementary machine gives half of the torque value, plus a pulsating component with the same amplitude value, but with a frequency twice that of the speed rotating frequency. These classical results show how the implicit mechanical linkage between the two fictive machines eliminates the pulsating component.

3.4 The *d-q* synchronous reference frame

Park's transformation is defined by:

$$[f_{abc}] = [T_3] \cdot [f_{dq0}],\ \ and\ \ [f_{dq0}] = [T_3^{-1}] \cdot [f_{abc}]$$

$$with\ \ T_3 = \sqrt{\frac{2}{3}} \cdot \begin{bmatrix} \cos(\theta_e) & -\sin(\theta_e) & 1/\sqrt{2} \\ \cos\left(\theta_e - \frac{2\pi}{3}\right) & -\sin\left(\theta_e - \frac{2\pi}{3}\right) & 1/\sqrt{2} \\ \cos\left(\theta_e - \frac{4\pi}{3}\right) & -\sin\left(\theta_e - \frac{4\pi}{3}\right) & 1/\sqrt{2} \end{bmatrix},$$

$$and\ \ T_3^{-1} = \sqrt{\frac{2}{3}} \cdot \begin{bmatrix} \cos(\theta_e) & \cos\left(\theta_e - \frac{2\pi}{3}\right) & \cos\left(\theta_e - \frac{4\pi}{3}\right) \\ -\sin(\theta_e) & -\sin\left(\theta_e - \frac{2\pi}{3}\right) & -\sin\left(\theta_e - \frac{4\pi}{3}\right) \\ 1/\sqrt{2} & 1/\sqrt{2} & 1/\sqrt{2} \end{bmatrix} \tag{11}$$

Fig.6 presents the Causal Ordering Graph of the electrical part in the synchronous reference frame:

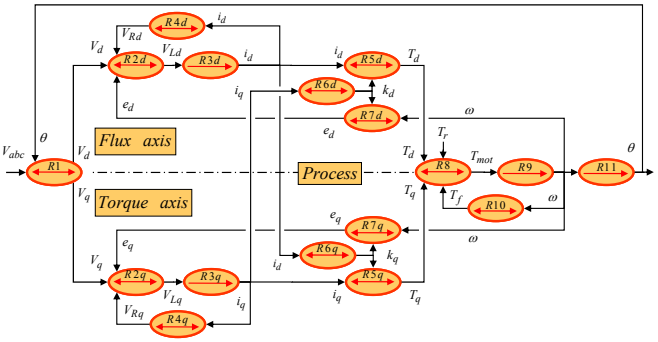

Fig.6: COG of the electrical part of a PMSM in (*d-q*)

The different relations for the flux axis are given by:

$$R2d \rightarrow V_{Ld} = V_d - e_d - V_{Rd},\ R7d \rightarrow e_d = k_d \cdot \omega$$

$$R3d \rightarrow L_d \cdot \frac{d}{dt} i_d = V_{Ld},\ R4d \rightarrow V_{Rd} = R \cdot i_d$$

$$R5d \rightarrow T_d = k_d \cdot i_d,$$

$$R6d \rightarrow k_d = -N_p \cdot (L_q \cdot i_q)$$

The different relations for the torque axis are given by:

$$R2q \rightarrow V_{Lq} = V_q - e_q - V_{Rq},\ R7q \rightarrow e_q = k_q \cdot \omega$$

$$R3q \rightarrow L_q \cdot \frac{d}{dt} i_q = V_{Lq},\ R4q \rightarrow V_{Rq} = R \cdot i_q$$

$$R5q \rightarrow T_q = k_q \cdot i_q$$

$$R6q \rightarrow k_q = N_p \cdot \left(L_d \cdot i_d + \sqrt{3/2} \cdot \hat{\phi}_f \right)$$

Wherein:

$$[L_{dq}] = \begin{bmatrix} L_d & 0 \\ 0 & L_q \end{bmatrix},\ \ with\ \ L_d = L_q = L - M \tag{12}$$

The *R*1 processor represents Park's transformation matrix described in (11). The benefits of Park's transformation are the conversion of the sinusoidal values of voltage, fluxes and currents into constant values, which facilitate the controller design. That is represented in Fig.6 with the interaction in the *R*1 processor of the electrical angle. So, this sinusoidal envelop is reported

outside the electrical model in the *R*1 processor, as a simple transformation operator.

The *R*8 processor includes the torque expression, which is defined from two elementary machines (13). We can notice that the direct axis *d* represents the flux axis, and the quadrature axis *q* represents the torque axis. Finally, we can notice that each machine looks like a DC motor.

$$T_{em} = T_d + T_q = \phi_d \cdot i_q - \phi_q \cdot i_d \qquad (13)$$

The *R*5*d*, and *R*7*d* processors denote a gyrator. The gyrator in COG formalism is used as a symbol of all electromechanical conversions. The variables of dual energy nature are modulated by a coefficient *k* that is characteristic of the object; the gyrators associate processors of comparable energy nature. Here, the coefficients k_d and k_q are defined by the *R*6*d* and *R*6*q* processors respectively. The disadvantage of Park's transformation is that the coefficients k_d and k_q needed for the gyrator denote a cross coupling between the two axes. Consequently, in the controller design, the control of these flux loops will be more complicated, especially in case of saturation.

3.5 Conclusion

We have obtained electrical models in the stationary reference frame (*abc*) and in Concordia's reference frame (α-β). The Causal Ordering Graph of each model has exactly the same structure. Evidently, processor relations are different, depending on the applied transformation matrix. So, in the stationary reference frame, the three currents are sinusoidal with an offset of $2\pi / 3$ on each other. Thus, for a closed-loop control strategy, controllers have to compensate error on sinusoidal signals.

In Concordia's reference frame, there are only two sinusoidal currents in quadrature. So, two controllers only will be required to design the torque control loop.

Finally, we have obtained an electrical model in Park's reference frame. The two currents i_d and i_q are constant at a constant speed. But only one current i_q is really needed to assume the torque control. Indeed, if the second current i_d is settled to zero, then the torque turns into $T_{em} = K * i_q$, which will clearly reduce the control structure.

4 Rotary / linear motor analogy

4.1 Structure of a linear synchronous motor

Fig.7 represents an example of PM linear synchronous motor geometry: A LIMES400/120 by Siemens.

The moving part is called the forcer. It's composed of a three-phase winding called the primary. τ_p represents a pole pitch step between two consecutive magnetic poles of the secondary [18].

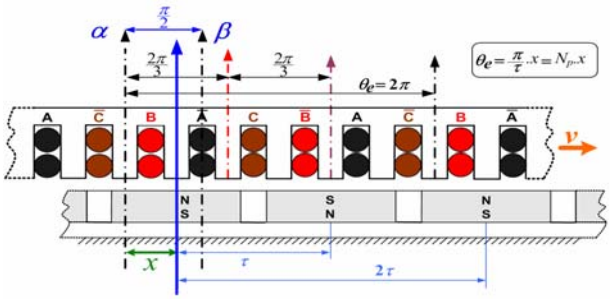

Fig.7: Principle schematics of a PMLSM (Siemens)

4.2 Principle of the rotary / linear analogy

For a rotary motor, the three armature windings are each shifted by an electrical angle of $2\pi / 3$, and each winding covers an electrical angle of π in the stationary reference. By analogy, the stator armature windings of a PMLSM are each shifted by a distance of $2\tau_p / 3$, and every winding covers a distance of τ_p in the linear reference frame.

The electrical angle along which the primary of the PMLSM moves in the linear reference frame can be expressed by:

$$\theta_e = N_p \cdot x, \quad with \quad N_p = \frac{\pi}{\tau_p} \qquad (14)$$

Here, N_p is the electrical position constant of the PMLSM. Equivalences of the electrical angle and the electrical angular speed between rotary motors and PMLSMs are shown in Table 1.

Table 1: Equivalences of electrical angle and electrical angular speed between rotary motors and PMLSMs

Parameter name	**Rotary motor**	**PMLSM**
Electrical angle (θ_e)	$\theta_e = N_p \cdot \theta$	$\theta_e = N_p \cdot x$
Electrical angular speed (ω)	$\omega = N_p \cdot \Omega$	$\omega = N_p \cdot v$

Classically in machine tool applications, the linear motors are star-connected with an inaccessible neutral wire: only two currents are independent. Thus, the (α-β) reference frame is more appropriate to represent such systems.

4.3 More detailed model

In this section, we can go further into our PMLSM model. Indeed, among the assumptions we have taken, we have considered that the geometry of a linear motor is the same as that of a rotary motor.

Models of linear motors can be different with models of rotary motors [18]. Thus, for example, we can find:

1) Longitudinal end-effects forces are added to cogging forces, which turn into detent forces:

$$R12 \rightarrow T_{det} = \hat{T}_{cog} \cdot \sin(6N_p \cdot \theta) + \hat{T}_{ext} \cdot \sin(2N_p \cdot \theta) \qquad (15)$$

2) Back-electromotive forces have harmonics mutation, as in the R6 processor of Fig.5 [19]:

$$R6 \rightarrow \frac{d\phi_{\alpha\beta}}{dx} = \sqrt{\frac{3}{2}} \cdot N_p \cdot \hat{\phi}_f \sum_{n=1}^{\infty} \begin{bmatrix} K_{\alpha}^{2n-1} \cdot \sin\left[(2n-1)N_p \cdot x\right] \\ K_{\beta}^{2n-1} \cdot \cos\left[(2n-1)N_p \cdot x\right] \end{bmatrix} \qquad (16)$$

3) Balanced inductances (1) are changed to unbalanced inductances [20]:

$$\left[L_{abc}\right] = \begin{bmatrix} L & M_1 & M_1 \\ M_1 & L & M_2 \\ M_2 & M_2 & L \end{bmatrix} \qquad (17)$$

5 Conclusion

In this paper, we have presented the modelling of a synchronous motor in order to design an optimal control structure. This Part I present the electrical model of a PMSM in the (*abc*) reference frame, the (*α-β*) stationary reference frame and the (*d-q*)reference frame. Each time, the Causal Ordering Graph (COG) formalism has been applied to analyse the waveforms and the interactions between the voltages, the currents and the fluxes. We have shown that our models can be used with rotary and linear synchronous motors. Some of the specificities of linear motors have been explained. In Part II, we present the control design by applying the inversion principle of the COG of our PMLSM models.

References:

[1] S.E. Lyshevski, *Electromechanical Systems, Electric Machines, and Applied Mechatronics*, CRC Press, 1999.

[2] H.A. Toliyat, S. Campbell, *Dsp-Based Electro-mechanical Motion Control*, CRC Press, 2003.

[3] X. Guillaud, P. Degobert, J.P. Hautier, Modelling Control and Causality: The Causal Ordering Graph, *16th IMACS Control Engineering Lausanne* (CD Rom), August 2000.

[4] Y. Iwasaki, H.A. Simon, Causality in device behaviour, *Artificial Intelligence 29*, Elsevier Science Publishers, 1986, pp.3-32.

[5] Y. Iwasaki, H.A. Simon, Causality and model abstraction, *Artificial Intelligence 67*, Elsevier Science Publishers, 1994, pp.143-194.

[6] J. Kleer, J.S. Brown, Theories of causal ordering, *Artificial Intelligence 29*, Elsevier Science Publishers, 1986, pp.33-61.

[7] G. Dauphin-Tanguy, S. Scavarda, *Physical systems modelling by Bond-graphs*, Tome 1 (in French), Masson, 1993.

[8] P.C. Breedveld, Fundamentals of bond graphs, *In IMACS annals of computing and applied mathematics*, Modelling and simulation of systems, Vol.3, 1989, pp.7–14.

[9] G. Dauphin-Tanguy, *Bond-graphs*, Hermes Science, 2000.

[10] D. Karnopp, R. Rosenberg, *Systems dynamics: a unified approach*, John Wiley & Sons, 1975.

[11] D. Karnopp, D. Margolis, R. Rosenberg, *Systems dynamics: modelling and simulation of mechatronic systems*, John Wiley & Sons, 2000.

[12] J.P. Hautier, P.J. Barre, The Causal Ordering Graph - A tool for system modelling and control law synthesis, *Studies in Informatics and Control*, Dec. 2004, Vol.13, No.4, pp.265-283.

[13] P.C. Krause, *Analysis of electrical machinery*, Springer-Verlag, McGraw-Hill Book Company, New-York, 1987.

[14] A.E. Fitzgerald, C. Kingsley, S.D. Umans, *Electric Machinery*, McGraw-Hill, 6th ed., 1990, pp.248–252.

[15] B. Armstrong-Helouvry, P. Dupont, C. Canudas de Wit, A Survey of Models, Analysis Tools and Compensation Methods for the Control of Machines with Friction, *Automatica*, Vol.30, No.7, July 1994.

[16] N. Bianchi, S. Bolognani, Design techniques for reducing the cogging torque in surface-mounted PM motors, *Industry Applications, IEEE Transactions on*, Vol.38, No.5, Sep. 2002, pp.1259-1265.

[17] C. Concordia, *Synchronous Machines*, Wiley and Son, New York, 1951.

[18] J.F. Gieras, Z.J. Piech, *Linear Synchronous Motors, Transportation and Automation Systems*, CRC Press, Sep. 1999.

[19] G. Remy, A. Tounzi, P.-J. Barre, F. Piriou, J.-P. Hautier, Finite-Element Analysis of Non-Sinusoidal Electromotive Force in a Permanent Magnet Linear Synchronous Motor, *The Fifth International Symposium on Linear Drives for Industry Applications*, LDIA2005, Kobe-Awaji, Japan, 25-28 Sept. 2005.

[20] P.J. Barre, A. Tounzi, J.P. Hautier S. Bouaroudj, Modelling and thrust control using resonating controller of asymmetrical PMLSM, *9th European Conference on Power Electronics and Applications*, EPE2001, Graz, 27-29 August, 2001.